Hydration of Copper(II): New Insights from Density Functional Theory and the COSMO Solvation Model

Vyacheslav S. Bryantsev,[†] Mamadou S. Diallo,[†,‡] Adri C. T. van Duin,[†] and William A. Goddard III*,[†]

Materials and Process Simulation Center, Beckman Institute 139-74, California Institute of Technology, Pasadena, California 91125, and Department of Civil Engineering, Howard University, Washington, D.C. 20059

The hydrated structure of the Cu(II) ion has been a subject of ongoing debate in the literature. In this article, we use density functional theory (B3LYP) and the COSMO continuum solvent model to characterize the structure and stability of $[Cu(H_2O)_n]^{2+}$ clusters as a function of coordination number (4, 5, and 6) and cluster size ($n = 4-18$). We find that the most thermodynamically favored Cu(II) complexes in the gas phase have a very open four-coordinate structure. They are formed from a stable square-planar $[Cu(H_2O)_8]^{2+}$ core stabilized by an unpaired electron in the Cu(II) ion $d_{x^2-y^2}$ orbital. This is consistent with cluster geometries suggested by recent mass-spectrometric experiments. In the aqueous phase, we find that the more compact five-coordinate square-pyramidal geometry is more stable than either the four-coordinate or six-coordinate clusters in agreement with recent combined EXAFS and XANES studies of aqueous solutions of Cu(II). However, a small energetic difference ($\sim$1.4 kcal/mol) between the five- and six-coordinate models with two full hydration shells around the metal ion suggests that both forms may coexist in solution.

1. Introduction

Knowledge of local coordination environment around Cu(II) in aqueous solutions is essential for understanding the structures and functions of copper-containing proteins.[1−5] Detailed information on ligands arrangement around the Cu(II) ion is only available in the solid state[6−13] whereas the structural information in the aqueous phase[13−20] is less definitive and available only for few Cu^{2+} complexes. Although static[20−30] and dynamic[31−37] electronic structure calculations can, in principle, provide such information, realistic modeling of Cu(II) complexes in aqueous solution with highly flexible coordination environment still remains a challenge. Classical force field simulations [even with three-body potential functions[35]] do not provide good alternatives to electronic structure calculations in this case, as they fail to describe the Jahn−Teller distortion around the aqueous Cu^{2+} ion unless explicit ligand field correction terms stabilizing the distorted octahedral Cu(II)−water clusters are employed.[10]

The electronic term (or adiabatic potential) for the $3d^9$ configuration of Cu^{2+} in the symmetrical octahedral environment (O_h point group) is 2-fold degenerate.[38,39] According to the Jahn−Teller theorem,[40,41] it has no minimum with respect to certain nuclear displacements. Taking into account quadratic terms of vibronic interaction leads to preferential distortion of the octahedral coordination geometry along one of the three 4-fold axes.[41] Figure 1 shows a schematic representation of the splitting of d-electron energy levels resulting from the withdrawal of two axial ligands from the regular octahedral ligand field.

One of the important consequences of Jahn−Teller distortion for Cu^{2+}(aq) is a high mobility of the axial ligands and fast
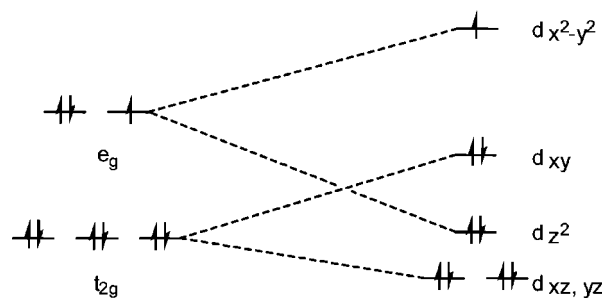
Figure 1. Crystal field splitting diagram of the 3d orbitals in Cu(II) by the withdrawal of two axial ligands.

first-shell ligand exchange dynamics. The rate of exchange of water molecules in the first shell around Cu^{2+} from the destabilized axial positions is 4.4×10^9 s^{-1} ($T = 298$ K), as estimated using the ^{17}O NMR technique.[42,43] It is several orders of magnitude faster than that of any other first-row divalent transition metal ion. Another direct consequence of the Jahn−Teller effect is the flexibility (plasticity) of the coordination geometry of Cu(II) which can adopt a variety of coordination geometries in the crystalline phase.[6−13] For example, crystal structures of Cu(II)−amino acids complexes with four-, five-, and six-coordinate geometries are all common, suggesting that energetic differences between them are small. Consistent with the Jahn−Teller effect, many of these structures include irregular or distorted coordination geometries.

Surprisingly, there is still ongoing debate on the coordination environment for the hydrated Cu(II) complex. Structural analysis in the solid state [recently revisited by Persson et al.[13] using EXAFS spectroscopy] showed that the local structures of known $[Cu(H_2O)_6]^{2+}$ complexes are consistent with the elongated octahedral configuration. Note that previously reported regular octahedral coordinations for $[Cu(H_2O)_6](BrO_3)_2$ and $[Cu(H_2O)_6]SiF_6$ were attributed to structural disorder in the

* Corresponding author. Phone: 626 395 2730. Fax: 626 585 0918. E-mail: wag@wag.caltech.edu.
† California Institute of Technology.
‡ Howard University.

Hydration of Copper(II)

J. Phys. Chem. A, Vol. 112, No. 38, 2008 **9105**

TABLE 1: Basis set Dependence of Relative Energies (kcal/mol) for $[Cu(H_2O)_{10}]^{2+}$ Conformers

conformer[a]	LACVP/6-31G(d,p)	LACV3P/6-311G(d,p)[b]	LACVP+/6-31++G(d,p)	LACV3P+/6-311++(d,p)	LACV3P+(2f)/aug-cc-pVTZ(-f)[c]
10w-a	0.00	0.00	0.00	0.00	0.00 (0.00)
10w-b	−0.30	0.22	1.46	1.22	1.07 (1.04)
10w-c	6.45	5.98	7.76	7.48	7.61 (7.28)
10w-d	−1.64	−1.05	1.55	1.45	1. 09 (1.21)
10w-e	6.33	6.91	9.72	10.36	9.67 (9.60)

[a] The structures of the complexes are shown in Figure 2. [b] The standard Los Alamos effective core potential (LACVP) uncontracted to form a triple-ζ valence basis set, LACV3P.[61] [c] The LACV3P+ basis set augmented by two f-polarization functions (α_f = 4.97 and 1.30) on Cu, LACV3P+(2f).[27] The values in parentheses are LACV3P+(2f)/aug-cc-pVTZ(-f) single point energies on LACV3P+/6-311++(d,p) optimized geometries.

crystal lattice masking the tetragonally distorted symmetry. In contrast, structural chararacterization of aqueous solutions of Cu(II) have not been conclusive to date. Pasquarello et al.[12] [on the basis of combined neutral diffraction and first-principles molecular dynamics simulations] questioned the classical 6-fold octahedral geometry around Cu(II) and suggested that transformations between the five-coordinate regular square pyramidal and trigonal bipyramidal configurations occur in solution. This view, however, has not been supported by subsequent X-ray-absorption spectroscopy (XAS).[13,18−20] Analysis of the extended X-ray absorption fine structure (EXAFS) spectra of aqueous solutions of Cu(II) by Persson et al.,[13] Benfatto et al.,[18] and Frank et al.[20] indicated that the best fit to the experimental data can be achieved using either a distorted square pyramidal or a distorted octahedral coordination. Persson et al.[13] selected the latter geometry based on a marginally better fit of wide-angle X-ray scattering (WAXS) data of aqueous solutions of Cu(II). Conversely, Benfatto et al.[18] and Frank et al.[20] analyzed the XANES portions of the XAS spectra of Cu(II)−water solutions and concluded that a square-pyramidal model with one elongated axial water molecule provides a better fit of the data than a four-coordinate model or a Jahn−Teller axially elongated six-coordinate model. More recently, Chaboy et al.[19] used two absorption channels for simulating the EXAFS and XANES spectra of Cu(II)−water solutions. They concluded that the four-, five-, and six-coordinate structures are indistinguishable and are likely to dynamically coexist in solution.

The theoretical calculations carried out to date have not been able to resolve this debate convincingly. Two independent Car−Parrinello molecular dynamics (MD) simulations performed [using the BLYP functional and a plane-wave basis set] predicted a 5-fold coordination for Cu²⁺.[31,32] In contrast, QM/MM MD simulations [employing HF, B3LYP, and MP2 levels of theory with the double-ζ valence basis set for water and the comparable LANL2DZ basis set for Cu²⁺] resulted in predicting exclusively the Jahn−Teller distorted 6-fold coordinated species.[34−37]

A study of the hydration of Cu²⁺ by a small number of water molecules may be an important step toward a better understanding of peculiar solvation effects in bulk water. Electronic structure calculations and mass-spectrometric analysis provide convenient tools for studying metal ion−H₂O clusters[44] in the gas phase. There is often assumed to be a relationship between the most intense peak in the mass-spectra and the ion cluster composition including the first shell of solvent molecules around an ion. For Cu²⁺, however, the most intense signal corresponds to the cluster containing eight water molecules.[45,46] Bérces et al.[24] attributed this observation to the stabilization of a planar structure, consisting of four water molecules in the first shell with additional four water molecules in the second shell located at the corners of a square and bound by means of two charge-enhanced hydrogen bonds. Stace and co-workers[47] have recently

performed a detailed mass spectrometric study on $[Cu(H_2O)_n]^{2+}$ complexes. They suggested that a very open structure stabilized by a 2-D array of hydrogen bonds may be highly plausible even for $n \geq 19$. The majority of previous electronic structure calculations,[20−22,24,27] however, have been limited to the study of hydrated copper clusters with $n \leq 8$. Thus, the effect of the full second and consequent shells of water on electronic structure, solvation structure and thermodynamics of $[Cu(H_2O)_n]^{2+}$ has not been considered in much detail in previous theoretical studies of Cu(II)−water complexes.

In this article, we present a cluster-continuum perspective of the structural, energetic, and thermodynamic aspects of Cu²⁺ hydration. Electronic structure calculations are used to determine stable geometries and relative energies of four-, five-, and six-coordinate $[Cu(H_2O)_n]^{2+}$ complexes as a function of cluster size, with $n = 4–18$. A COSMO solvation model[48] is applied to simulate the effect of the outer solvation region. In agreement with recent experimental observations,[18,20,47] our calculations suggest preference for coordination number four in the gas phase and coordination number five in the aqueous phase for $n \geq 8$. The results firmly establish the nature of the interactions of Cu²⁺ with equatorial and axial water ligands. The latter are bound to Cu²⁺ by primarily electrostatic interactions that are weaker than individual charged-enhanced hydrogen-bonding interactions in the outer region across all cluster sizes ($n = 5 − 18$). The calculated solvation free energy of Cu²⁺ using our mixed cluster/continuum model shows good agreement with the experimental value.

2. Computational Methods

Electronic structure calculations in the gas phase were performed with the Jaguar 7.0 quantum chemistry software.[49] DFT calculations were carried out using Becke's[50] three-parameter functional and the correlation function of Lee, Yang, and Parr[51] (B3LYP). The application of the B3LYP method to metal ion−water systems has proved a reasonable success.[52−55] For open-shell Cu²⁺−ligand systems with low coordination numbers ($n = 1, 2$) it has been reported[56−58] that B3LYP binding energies are overestimated compared to CCSD(T) results. However, the B3LYP relative energies for systems with similar spin density distribution are in good agreement with those determined by highly correlated electronic structure methods.[56,59] Table 1 shows the effect of basis set size on the relative energies of $[Cu(H_2O)_{10}]^{2+}$ conformers. The results suggest that diffuse functions are necessary to capture the relative energetic stabilities of these complexes. The geometries of all complexes were optimized using the standard 6-311G++(d,p) basis set with diffuse functions for the light atoms and the standard Los Alamos effective core potential LACVP[60] uncontracted to form a triple-ζ valence basis set, LACV3P,[61] and diffuse function for Cu. In addition, single-point energy calculations were
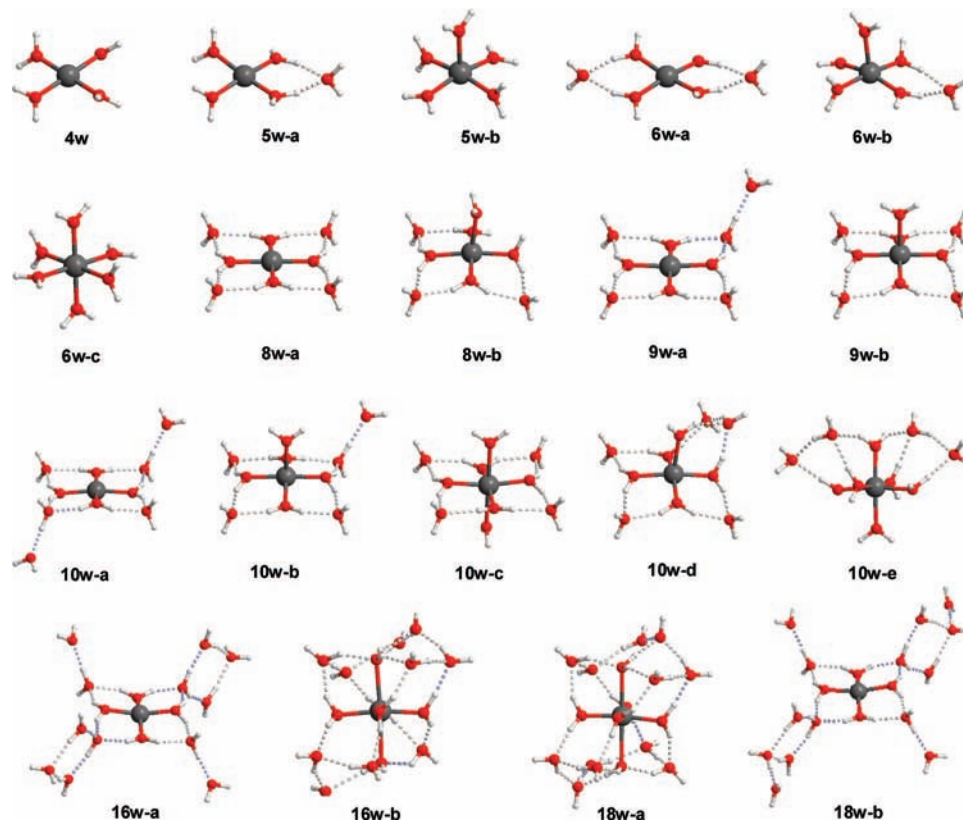
Figure 2. Gas-phase structures of $[Cu(H_2O)_n]^{2+}$ optimized at the B3LYP/LACV3P+/6-311++(d,p) level of theory.

performed using more extended basis sets, namely the aug-cc-pVTZ(-f) basis set[62] on the light atoms and the LACV3P+ basis set augmented by two f-polarization functions[27] ($\alpha_f = 4.97$ and 1.30) on Cu. Control calculations for $[Cu(H_2O)_{10}]^{2+}$ complexes show that this procedure leads to small differences in relative energies (0.03–0.33 kcal/mol) when compared to results obtained after full optimization at the B3LYP/LACV3P+(2f)/aug-cc-pVTZ(-f) level (Table 1). Vibrational frequencies were computed analytically at the B3LYP/LACVP/6-31G(d,p) level unless otherwise indicated. The standard Gibbs free energy of each species in the gas phase was calculated using the standard rigid rotor-harmonic oscillator approximation without scaling.

Coordination and thermodynamic properties of Cu^{2+} in bulk water were modeled by explicit inclusion of water molecules in the vicinity of the metal ion and implicit treatment of the rest of the solvent with dielectric continuum models. Such mixed cluster/continuum models[63–85] are preferred over pure dielectric continuum models when dealing with ionic solutes that have concentrated charge densities with strong local solute–solvent interactions.

Solvation calculations for ionic clusters were carried out using the COSMO dielectric continuum model[48] implemented in Turbomole,[86] with geometries fully optimized in the solvent reaction field at the B3LYP/LAV3P+/6-311++G(d,p) level. COSMO calculations were carried out using the recommended solvation parameters optimized for neutral solutes:[87] solvent probe radius of 1.3, solvent dielectric constant of 78.4, and atomic radii of 1.30 Å for hydrogen and 1.72 Å for oxygen. The nonelectrostatic component (e.g., cavity term) of the solvation free energy was estimated using the empirical relation given in ref 88. It has been shown[85] that COSMO model accurately reproduces the experimental hydration free energy of water (within ~0.3 kcal/mol), which is critical for accurate calculations of solvation free energies of charged solutes using

mixed cluster/continuum models. The Bondi radius,[89] scaled by 1.17 (2.223 Å) was employed for copper. The results are not sensitive to the choice of this parameter if the metal ion is completely surrounded by water molecules.

3. Results and Discussion

3.1. Structure and Energetics of $[Cu(H_2O)_n]^{2+}$ in the Gas Phase. We carried out an extensive search for the low-lying isomers of $[Cu(H_2O)_n]^{2+}$ in the gas phase. Our objective was to analyze their stability as a function of the metal coordination number (4–6) and cluster size ($n = 4–18$). A strong preference of the hydrated Cu(II) ion to form very open structures by hydrogen bonding of the water molecules on the periphery of the complex allowed us to perform a systematic search of the plausible low-energy structures in the gas phase for $n \leq 18$ at the B3LYP/LACV3P+/6-311G++(d,p) level. The structures of the most stable $[Cu(H_2O)_n]^{2+}$ complexes for different coordination numbers are shown in Figure 2. Table 2 lists the electronic binding energies, binding free energies, and relative energies of these complexes. Table 3 summarizes the average Cu–water distances in the equatorial and axial positions of all studied complexes.

The Cu^{2+} cluster with four water molecules (**4w**) has a regular square-planar geometry. The water molecules are oriented to the ion by their dipole moments. The fifth water can coordinate to the axial position of copper (**5w-b**) or form two charge-assisted hydrogen bonds with water molecules in the first hydration shell (**5w-a**). The four-coordinate hydrogen-bonded geometry is energetically preferred by 2.3, 3.5, and 4.1 kcal/mol for $n = 5$, 6, and 8, respectively. Binding of two water molecules in the axial positions (**6w-c**) is significantly less favorable (by 9.1 kcal/mol) compared to hydrogen-bonding interaction with the water in the primary hydration shell (**6w-a**). A planar $[Cu(H_2O)_8]^{2+}$ unit (**8w-a**) stabilized by the network

Hydration of Copper(II)

J. Phys. Chem. A, Vol. 112, No. 38, 2008 **9107**

TABLE 2: Electronic Binding Energies ($\Delta E_{0K,bind}$), Gas-Phase Binding Free Energies ($\Delta G^o_{g,bind}$), Solvation Energies (ΔG^*_{solv}), and Relative Electronic Energies in the Gas Phase ($\Delta E_{0K,rel}$) and in Aqueous Solution ($\Delta E_{rel}(aq)$) for $[Cu(H_2O)_n]^{2+}$ Complexes with Four, Five, and Six Water Molecules in the First Coordination Shell (in kcal/mol)

structure[a]	c.n.[b]	$\Delta E_{0K,bind}$[c]	$\Delta G^o_{g,bind}$[d]	ΔG^*_{solv}[e]	$\Delta E_{0K,rel}$	$\Delta E_{rel}(aq)$
4w	4	−309.72	−270.02	−208.23		
5w-a	4	−339.58	−286.00	−195.44	0.00	0.00
5w-b	5	−337.30	−285.87	−196.71	2.28	1.01
6w-a	4	−367.48	−299.49	−185.04	0.00	0.00
6w-b	5	−363.99	−298.88	−187.10	3.49	1.43
6w-c	6	−358.37	−295.80	−188.95	9.11	5.19
8w-a	4	−415.30	−323.69	−165.65	0.00	0.67
8w-b	5	−411.18	−319.96	−170.44	4.12	0.00
9w-a	4	−432.05	−330.66	−160.01	0.00	3.11
9w-b	5	−431.20	−328.78	−163.98	0.86	0.00
10w-a	4	−448.33	−335.52[f]	−154.25	0.00	5.26
10w-b	5	−447.29	−334.96	−158.28	1.04	2.28
10w-c	6	−441.05	−330.42	−159.97	7.29	6.83
10w-d	5	−447.12	−331.82	−160.73	1.22	0.00
10w-e	6	−438.74	−323.25	−163.65	9.60	5.46
16w-a	4	−528.46	−348.70[f]	−140.16	0.00	5.94
16w-b	6	−527.36	−334.60	−147.19	1.09	0.00
18w-a	6	−553.99	−337.63	−145.33	0.00	0.00
18w-b	4	−551.38	−349.42[f]	−138.02	2.61	9.92

[a] The structures of the conformers are shown in Figure 2. [b] Coordination number. [c] B3LYP/LACV3P+(2f)/aug-cc-pVTZ(-f) single point energies on B3LYP/LACV3P+/6-311G++(d,p) optimized geometries. [d] ZPE and thermal corrections calculated at the B3LYP/LACVP/6-31G(d,p) level. [e] Solvation free energies obtained after geometry optimization at the COSMO-B3LYP/LACV3P+/6-311G++(d,p) level. [f] Vibrational frequencies were computed numerically, all of which are real. Small imaginary frequencies (<20 cm^{-1}) were obtained using the analytical Hessian. These imaginary frequencies reflect floppy modes of dangling water molecules and could be due to numerical noise.

TABLE 3: Equatorial and Axial Cu−O Distances (Å) in $[Cu(H_2O)_n]^{2+}$

structure	gas phase		implicit solvent	
	r_{Cu-Oeq}	r_{Cu-Oax}	r_{Cu-Oeq}	r_{Cu-Oax}
4w	1.976		1.961	
5w-a	1.973		1.963	
5w-b	2.011	2.181	1.994	2.171
6w-a	1.969		1.965	
6w-b	2.005	2.209	1.997	2.206
6w-c	2.033	2.255; 2.225	2.020	2.247; 2.250
8w-a	1.952		1.959	
8w-b	1.994	2.241	1.999	2.238
9w-a	1.951		1.960	
9w-b	1.991	2.216	1.996	2.239
10w-a	1.950		1.955	
10w-b	1.990	2.221	1.997	2.237
10w-c	2.013	2.317; 2.317	2.009	2.340; 2.345
10w-d	2.000	2.216	2.004	2.250
10w-e	2.024	2.287; 2.289	2.025	2.283; 2.297
16w-a	1.949		1.954	
16w-b	2.009	2.437; 2.442	2.014	2.409; 2.416
16w-c(aq)[a]			2.005	2.221
18w-a	2.005	2.470; 2.494	2.016	2.437; 2.447
18w-b	1.949		1.954	
18w-e(aq)[a]			2.001	2.273

[a] The lowest energy five-coordinate square-pyramidal structures in the aqueous phase. The corresponding gas-phase structures are not stationary points and rearrange to more stable six-coordinate elongated octahedral geometries.

of hydrogen bonds has been given special significance[24,44,47] because of the appearance of the most intensive mass spectral peak at $n = 8$ for $[Cu(H_2O)_n]^{2+}$ ions in the gas phase.

We find that the stable eight-molecule square-planar unit (**8w-a**) is a key feature (i.e., a core) for many of the larger clusters. Structures of the complexes containing this core have the lowest electronic energy for $n \leq 16$ and the lowest standard Gibbs free energy for all $[Cu(H_2O)_n]^{2+}$ complexes with $n \leq 18$. Surprisingly, the most energetically favorable position for the ninth water is in the third hydration shell (**9w-a**), where a lone pair of oxygen is directed toward the hydrogen atom of the adjacent molecule in the second hydration shell. The conformation with the axial water (**9w-b**) is slightly higher in energy (0.9 kcal/mol). $[Cu(H_2O)_{10}]^{2+}$ has a similar preference for the four-coordinate structure (**10w-a**), which is 1.0 and 7.3 kcal/mol more stable compared to the lowest energy five-coordinate (**10w-b**) and six-coordinate (**10w-c**) complexes, respectively. Alternative geometries with a distorted **8w-a** unit (**10w-d**, **10w-e**) are energetically less stable in the gas phase. The propensity to form a third hydration shell at relatively small cluster sizes is consistent with a recent study of Williams et al.,[90] attributing IR spectral features for $[Cu(H_2O)_{10-12}]^{2+}$ to clusters having single hydrogen bond acceptor water molecules.

The most stable conformation of $[Cu(H_2O)_{16}]^{2+}$, **16w-a**, is an open structure with the **8w-a** core, two four-membered rings, and two dangling waters and in the third hydration shell. Conversely, the lowest energy isomer of $[Cu(H_2O)_{18}]^{2+}$ has a compact 6-fold coordinated structure with Cu^{2+} fully surrounded by water (**18w-a**). It should be noted, however, that the higher

entropy of the sparse four-coordinate **18w-b** cluster compared to the more dense **18w-a** conformer favors the more open structure at 298.15 K. This behavior of the relatively large hydrated Cu^{2+} ions is unusual; many solvated metal dications adopt more compact geometries that can accommodate a larger number of hydrogen bonds. However, it is fully consistent with a recent mass-spectrometric study of $[Cu(H_2O)_n]^{2+}$ by Stace and co-workers.[47] They reported charge reductions [through electron-capture induced dissociation by collision with Xe atoms] in copper−water clusters containing up to 19 water molecules. These experiments clearly demonstrated that hydrated Cu(II) complexes have very open structures that enable colliding Xe gas atoms to interact directly with the Cu^{2+} ion.

A valuable insight into coordination properties of Cu^{2+} in bulk water can be gained by analyzing the gas-phase binding energy of a water molecule coordinated in the axial and outer shell coordination sites as a function of cluster size (Figure 3). For this purpose, we performed additional calculations by forming an intermolecular bond with water in various vacant sites of $[Cu(H_2O)_n]^{2+}$, $n = 11-18$. Examples of $[Cu(H_2O)_{18}]^{2+}$ structures used to calculate water binding energies are shown in Figure 4. The geometries of all complexes optimized in the gas phase are provided in the Supporting Information. The strength of the interaction between $[Cu(H_2O)_n]^{2+}$ and an additional water molecule is expected to decreases with increasing cluster size, as illustrated in Figure 3. A surprising result is that the energy of the hydrogen bond between water molecules on the periphery of a Cu(II)−water complex is always stronger than the energy of water binding to the vacant axial sites on Cu^{2+}. Although the binding energy of the first axial water is comparable in magnitude to that of a hydrogen bond in a four-coordinate copper complexes, the binding of the second axial water is strongly disfavored for all n. For example, the energy cost for removing the second axial water in **18w-d** is 6.5 kcal/mol. Calculations for $[Cu(H_2O)_{22}]^{2+}$ (complex **22w** in Figure 4) show that the binding energy of the second axial water is
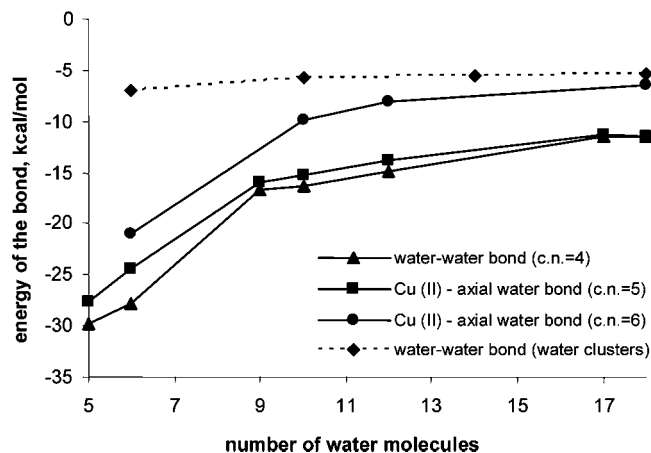
Figure 3. The dependence of the energy of the intermolecular water–water bond in four-coordinate complexes and of the Cu(II)–axial water bond in five- and six-coordinate complexes on the number of water molecules in $[Cu(H_2O)_n]^{2+}$. The dashed curve shows the average energy of the hydrogen bond in neutral water clusters.
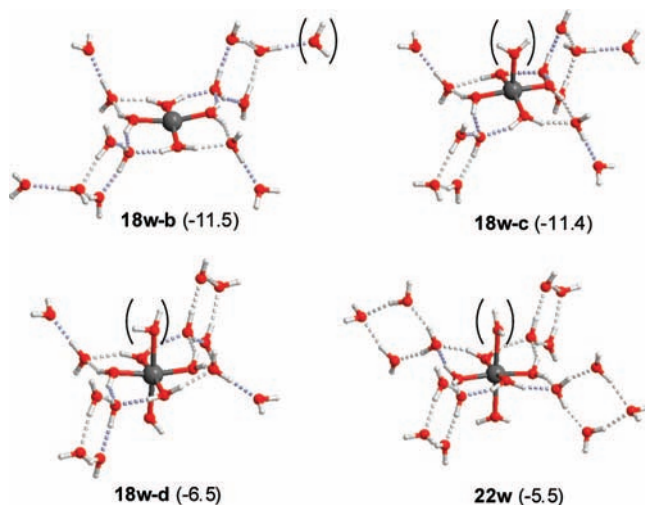

Figure 4. Structures and binding energies (kcal/mol) for coordination of a water molecule (shown in brackets) to the outer hydration shell and to the vacant axial sites in $[Cu(H_2O)_n]^{2+}$ ($n = 18, 22$). The binding energy for the axial water in **22w** is comparable to the strength of the hydrogen bond in neutral water clusters (see the dashed curve in Figure 3).

only 5.5 kcal/mol, which is similar to the strength of the hydrogen bond in neutral water clusters (see the dashed curve in Figure 3).[91] The overall results of these calculations suggest that one axial site on Cu²⁺ could easily be unoccupied in bulk water.

3.2. Analysis of Electron and Spin Distribution in $[Cu(H_2O)_n]^{2+}$. The much less favorable interaction of the axial ligands in the hydrated Cu(II) complexes can be understood by analyzing their electronic structure. Figure 5 shows representative β-LUMO orbital and spin density surfaces for the six-coordinate $[Cu(H_2O)_{10}]^{2+}$ complex, **10w-c**. This indicates that the unpaired electron density is primarily located on the Cu(II) $3d_{x^2-y^2}$ orbital and the σ-type lone-pair orbitals of the equatorial water molecules that can slightly overlap with each other. Conversely, water lone pairs in the axial positions experience repulsive interactions with the doubly occupied $3d_{z^2}$ orbital of Cu²⁺ that effectively screens the positive charge on the metal ion.

Natural atomic orbital (NAO) analysis[92,93] of charge distribution in aqua complexes of Cu(II) further indicates (Table 4)
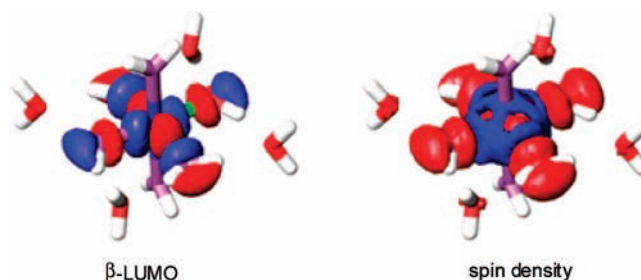
Figure 5. β-LUMO orbital and spin density for **10w-c**. The unpaired electron density is primarily located on the Cu²⁺ $d_{x^2-y^2}$ orbital and the equatorial H_2O σ-type lone pair orbitals.

TABLE 4: Natural Atomic Orbital (NAO) Charges (q) and Spin Densities (z) on Cu²⁺ and Water Molecules in the First Hydration Shell[a]

structure	$q_{Cu^{2+}}$	$q_{H_2O_{eq}}$	$q_{H_2O_{ax}}$	$z_{Cu^{2+}}$	$z_{H_2O_{eq}}$	$z_{H_2O_{ax}}$
4w	1.538	0.115		0.764	0.059	
5w-a	1.521	0.099		0.752	0.061	
5w-b	1.558	0.101	0.038	0.802	0.050	0.000
6w-a	1.510	0.085		0.748	0.062	
6w-b	1.533	0.091	0.036	0.781	0.054	0.000
6w-c	1.559	0.091	0.038	0.824	0.044	0.000
8w-a	1.505	0.069		0.740	0.064	
8w-b	1.502	0.075	0.031	0.759	0.060	0.000
9w-a	1.500	0.065		0.736	0.064	
9w-b	1.516	0.064	0.031	0.768	0.057	0.000
10w-a	1.492	0.061		0.731	0.066	
10w-b	1.507	0.060	0.030	0.763	0.058	0.000
10w-c	1.515	0.065	0.028	0.783	0.054	−0.001
10w-d	1.507	0.061	0.021	0.764	0.058	0.000
10w-e	1.501	0.076	0.019	0.781	0.055	−0.001
16w-a	1.469	0.047		0.714	0.070	
16w-b	1.465	0.058	0.012	0.756	0.061	0.000
18w-a	1.465	0.052	0.006	0.753	0.061	−0.001
18w-b	1.466	0.046		0.712	0.070	

[a] Average charges and spin densities on the equatorial and axial water molecules.

that the electron transfer from the equatorial water molecules to the Cu²⁺ is substantially larger ($0.046-0.115e$) than that from the axial water molecules ($0.006-0.038e$). Similarly, there is substantial spin density on the equatorial H_2O ($0.044-0.071e$), although it is essentially zero on the axial H_2O. These results confirm[27] that electron density from equatorial waters can be transferred to both the singly occupied $3d_{x^2-y^2}$ orbital and the lowest vacant 4s orbitals on Cu²⁺, whereas charge transfer from the axial waters is mostly limited to the Cu²⁺ 4s orbital.

Note that there is only a moderate variation of the NAO charge on Cu²⁺. This charge varies from $1.54e$ in the complex with four water molecules (**4w**) to $1.47e$ in the complex with eighteen water molecules (**18w-a**). However, as shown in Figure 6, the total charge on copper(II) and water molecules directly attached to the metal center drops considerably with the increasing size of a complex. Although this trend is not fully converged even at $n = 18$, it can be well approximated by the exponential decay function. The fact that charge transfer is not confined to the first coordination shell but significantly extends to the second and outer hydration shells has been also reported for the U(VI) complexes.[82,94] For soft divalent d- and f-block metal ions, this is likely to be a general phenomenon.

3.3. Structure and Energetics of $[Cu(H_2O)_n]^{2+}$ in the COSMO Dielectric Continuum Reaction Field. Solvation free energies and relative electronic energies of all complexes in aqueous solution were obtained after full geometry optimization in the COSMO solvent reaction field.[48] The results are sum-
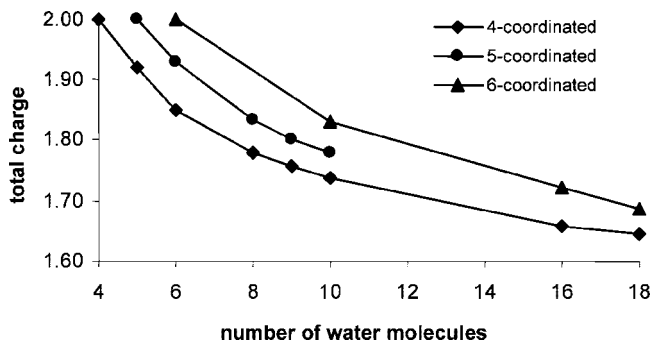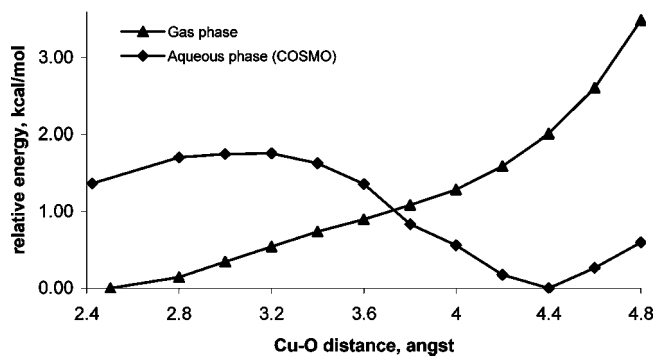
Figure 6. Dependence of the NAO charge confined by the first coordination shell around Cu^{2+} on the number of water molecules in $[Cu(H_2O)_n]^{2+}$. This indicates a significant charge transfer from the metal ion to the second and outer hydration shells.

Figure 7. Potential energy curves for moving one axial water molecule in the six-coordinate complex **18w-a** to the second hydration shell. This shows that in bulk water the six-coordinate Cu(II) complex is less stable than the five-coordinate complex, which is consistent with XANES.[18,20] Relative energies are obtained by geometry optimization at each Cu−O distance in the gas phase or in the field of the continuum solvent (COSMO model) at the B3LYP/LACV3P+/6-311++G(d,p) level of theory.

Figure 8. Potential energy curves for moving the axial water molecule in the five-coordinate complex **18w-e** to the second hydration shell. This shows that in bulk water the four-coordinate Cu(II) complex is less stable than the five-coordinate complex, which is consistent with EXAFS.[13,18,20] Relative energies are obtained by geometry optimization at each Cu−O distance in the gas phase or in the field of the continuum solvent (COSMO model) at the B3LYP/LACV3P+/6-311++G(d,p) level of theory.
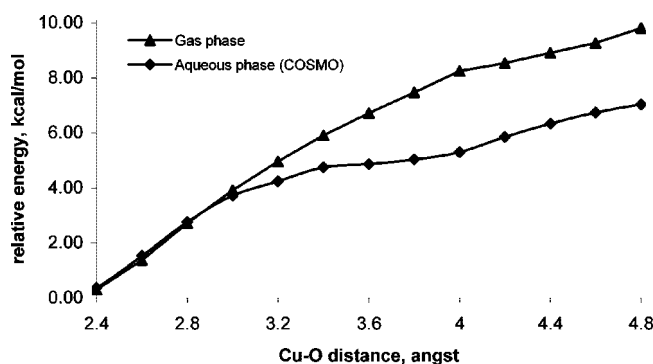
marized in Table 2. Generally, we find that the solvent reaction field increases the stability of the higher coordinated clusters, compared to their relative stabilies in the gas phase. Because of this, the five-coordinate geometry becomes the most stable geometry in the solvation phase for all $n \geq 8$. For example, the square-planar **8w-a** complex, which is considerably more stable than the five-coordinated **8w-b** complex in the gas phase, is predicted to be slightly less stable than the **8w-b** complex in the aqueous phase. If we compare $[Cu(H_2O)_{10}]^{2+}$ clusters with the same coordination number, we observe a transition from more open geometries in the gas phase (**10w-b**, **10w-c**) to more compact 3-D hydrogen-bonded structures in the aqueous phase (**10w-d**, **10w-e**). The most favored structure in the aqueous phase (**10w-d**) is stabilized through the formation of an additional hydrogen bond involving one axial water molecule at the expense of distorting the 2-D lattice of hydrogen bonds in the equatorial plane. Larger clusters have a clear preference for very compact structures in the water phase (**16w-b**, **18w-a**). Those structures that have the planar core and water molecules emanating from the central ion (**16w-a**, **18w-b**) have significantly higher energies.

As previously stated, the coordination numbers of solvated Cu(II) ions have been the subject of extensive debate in recent years.[14−20,31−37] Our calculations favor Cu(II)−water complexes with first-shell coordination number of five for clustes with eight to ten water molecules. Note the results of solvation calculations are sensitive to the selection of the copper solvation radius when Cu(II) ions are in contact with the solvent dielectric boundary. To avoid this problem, we performed a detailed analysis of the flexibility of the coordination environment in the six-coordinate **18w-a** cluster with full first and second hydration shells around the metal ion.

Potential energy curves for moving one axial water molecule in **18w-a** to the second hydration shell are shown in Figure 7. The displacement of an axial water molecule from its equilibrium position in **18w-a** results in a monotonic decrease of the stability of the complex in the gas phase. We find that the Cu−O_{ax} bond is very labile. The stretching of this bond by more than 1 Å leads to a decrease in binding energy by only ∼1 kcal/mol. What is even more remarkable is the character of this dependence in the high dielectric environment of water. The potential energy curve reveals a maximum at ∼3.0 Å and a global minimum at ∼4.4 Å. This result provides clear evidence in favor of the five-coordinate square-pyramidal model for the hydrated Cu(II) ion, which is 1.4 kcal/mol more stable than the 6-fold coordinated distorted octahedral structure at the B3LYP/LAV3P+/6-311++G(d,p) level. Qualitatively similar results have been also obtained for the **16w-b** complex. This result is

in agreement with the combined EXAFS and XANES analysis[20] of aqueous solutions of Cu(II) eliminating the competing four- and six-coordinate models for $[Cu(aq)]^{2+}$.

Note that using single-point energies at the B3LYP/LACV3P+(2f)/aug-cc-pVTZ(-f) level leads to a larger difference in relative stability between five- and six-coordinate complexes (2.6 kcal/mol in favor of the square-pyramidal coordination). Conversely, calculations with a basis set of double-ζ quality with no diffuse functions (LANL2DZ/6-31G**) reduce this difference to only 0.3 kcal/mol. A basis set of similar quality (LANL2DZ/DZP) has been employed previously[34−37] in the QM/MM molecular dynamics simulations of hydrated Cu^{2+}. Because small basis sets might not be sufficient to correctly describe the Cu^{2+}/H_2O systems, the reported fully atomistic QM/MM calculations[34−37] predicting 6-fold coordinated geometry of Cu^{2+} in water might need to be validated using more extended basis sets.

We also analyzed potential energy curves for the transformation of a 5-fold coordinated elongated pyramidal cluster to a 4-fold coordinated distorted square planar cluster. In this case, elongation of the Cu−O_{ax} bond leads to a monotonic increase in the relative energy of the complex in both gas and aqueous phases. The flexibility of the first axial water molecule is much lower than that of the second water due to stronger binding to

9110 *J. Phys. Chem. A, Vol. 112, No. 38, 2008*

Bryantsev et al.
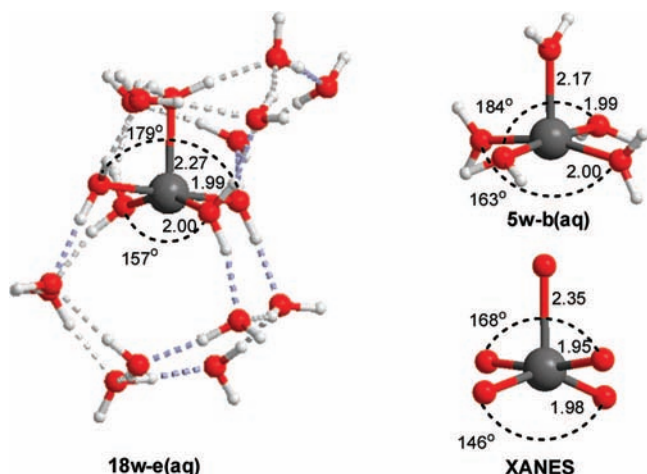
Figure 9. Comparison of the elongated five-coordinate square-pyramidal models for [Cu(aq)]$^{2+}$ obtained from COSMO-B3LYP calculations and the geometry obtained from the best fit to the XANES spectrum.[20]
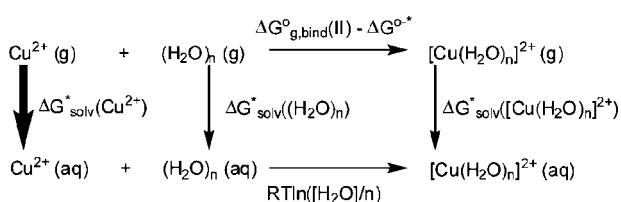
Figure 10. Thermodynamic cycle used in the calculation of $\Delta G^*_{solv}(Cu^{2+})$.

TABLE 5: Calculated Hydration Free Energy of Cu^{2+} Using the Thermodynamic Cycle Shown in Figure 10 (in kcal/mol)^a

n	$\Delta G^o_{g,bind}$ (II)	ΔG^*_{solv} ([Cu(H$_2$O)$_n$]$^{2+}$)	ΔG^*_{solv} ((H$_2$O)$_n$)	$\Delta G^{o \rightarrow *} - RT$ ln([H$_2$O]/n)	ΔG^*_{solv} (Cu^{2+})
6	−310.30	−185.04	−16.65	−3.21	−481.90
10	−355.01	−160.73	−21.31	−2.91	−497.34
18	−383.70	−146.70	−26.21	−2.56	−506.75

^{a} For calculation details see footnotes to Table 2.

the Cu(II) ion. The relatively high energy penalty for changing the number of water molecules in the first coordination shell from five to four (Figure 8) suggests that 4-fold coordinated clusters are not likely to exist in significant amounts in bulk water.

The structural parameters of our best model of [Cu(aq)]$^{2+}$ [i.e., **18w-e(aq)** with the lowest energy five-coordinate square-pyramidal geometry] in the water phase are shown in Figure 9. We compared this model to a cluster containing only five explicit water molecules (**5w-b(aq)**) and a geometrically unconstrained model that Frank et al.[20] used to carry out a full multiple scattering analysis of Cu(II)−water XANES spectra. We find that the presence of two hydration shells of water molecules around Cu^{2+} improves the overall agreement with the experimental structural parameters in comparison with the one-shell model. For example, the axial Cu−O$_{ax}$ bond distance in the large **18w-e(aq)** cluster (2.27 Å) is in satisfactory agreement with the XANES fitted value (2.35 ± 0.05 Å). Conversely, the smaller **5w-b(aq)** cluster has a much shorter axial Cu−O$_{ax}$ bond length (2.17 Å). This result is consistent with the value of 2.11 Å for the axial bond in [Cu(H$_2$O)$_5$]$^{2+}$ estimated by Frank et al.[20] using a spectroscopically calibrated hybrid DFT and the PCM continuum model. In all cases, B3LYP overestimates the equatorial Cu−O$_{eq}$ bond length by 0.025 Å.

3.4. Calculation of the Cu^{2+} Hydration Free Energy. Information on the thermodynamic stability of [Cu(H$_2$O)$_n$]$^{2+}$ collected in the previous sections can be used for the calculation of the solvation free energy of Cu^{2+} in water. An improved methodology for calculation of solvation free energies of charge solutes using mixed cluster/continuum solvent models has been recently described in ref 85. In this study, we employ the thermodynamic cycle shown in Figure 10 to calculate the hydration free energy of Cu(II). In Figure 10, $\Delta G^o_{g,bind}$(II) is the gas-phase free energy of complexation; ΔG^*_{solv}(X) is the standard free energy of solvation for X = Cu^{2+}, (H$_2$O)$_n$, and [Cu(H$_2$O)$_n$]$^{2+}$ and $\Delta G^{o \rightarrow *} = RT$ ln(24.46) = 1.89 kcal/mol (T = 298.15 K) is the free energy change of 1 mol of gas from 1 atm (24.46 L mol^{-1}) to 1 M (1 mol L^{-1}). Similarly, RT ln-([H$_2$O]/n) is the free energy change of 1 mol of (H$_2$O)$_n$ gas from 55.34/n M liquid state to 1 M. These are the standard state corrections that must be applied to bring each reactant or product in the upper and lower legs of the thermodynamic cycle to the same standard state (1M). From Figure 10, ΔG^*_{solv}(Cu^{2+}) can be expressed as

$$\Delta G^*_{solv}(Cu^{2+}) = \Delta G^o_{g,bind}(II) + \Delta G^*_{solv}([Cu(H_2O)_n]^{2+}) - \Delta G^*_{solv}((H_2O)_n) - \Delta G^{o \rightarrow *} - RT \ln([H_2O]/n) \quad (1)$$

The best estimate of the ΔG^*_{solv}(Cu^{2+}) can be obtained by analyzing the dependence of the right-hand side of eq 1 on the cluster size n. Table 5 summarizes the relevant thermodynamic parameters of the lowest energy aqueous-phase clusters, [Cu(H$_2$O)$_n$]$^{2+}$ and (H$_2$O)$_n$, n = 6, 10, and 18. The results shown in Table 5 indicate that the change in ΔG^*_{solv}(H$^+$) is very large from n = 6 to n = 10 (~15.4 kcal/mol) and smaller for n = 10 to n = 18 (~9.5 kcal/mol). Although we cannot claim that the calculated ΔG^*_{solv}(Cu^{2+}) have fully converged at n = 18, we can estimate ΔG^*_{solv}(Cu^{2+}) by extrapolating the calculated energies to $n \rightarrow \infty$ using the exponential fit. This yields a ΔG^*_{solv}($n \rightarrow \infty$) of −509.0 kcal/mol that is in excellent agreement with the experimental value of 507.0 ± 4 kcal/mol recommended by Tissandier et al.[95,96]

Note that the value of ΔG^*_{solv}(Cu^{2+}) calculated with only one solvation shell leads to an error of 27 kcal/mol (6 waters), whereas using two solvation shells leads to an accuracy of 2 kcal/mol (18 waters). The effect of decreasing ΔG^*_{solv}(Cu^{2+}) upon addition of water molecules in the outer shells can be ascribed to significant charge transfer involving ligands beyond the first hydration shell, as illustrated in Figure 6. Continuum dielectric models and classical molecular dynamics simulations with nonpolarizable potentials cannot describe this effect. Thus, explicit quantum mechanical modeling of the second hydration shell around divalent transition metal ions is critical for accurate prediction of their solvation free energies. Using more extended solvation layers might be necessary for trivalent and more highly charged metal ions.

4. Conclusions

In this article, we combine density functional theory (B3LYP) with a COSMO continuum solvent model to calculate the structures and energetic parameters of Cu(II)−water clusters. A key step was to locate the low-energy conformers for each coordination number (4−6) and cluster size (n = 4−18). The most favored Cu(II)−H$_2$O complexes in the gas phase have very open structures formed around a stable 4-fold coordinated square-planar [Cu(H$_2$O)$_8$]$^{2+}$ core. These open structures are consistent with cluster geometries suggested by recent mass-spectrometric experiments. We find that the energy of the

Hydration of Copper(II)

J. Phys. Chem. A, Vol. 112, No. 38, 2008 **9111**

hydrogen bond between water molecules on the periphery of a Cu(II)−water complex is stronger than the energy of water binding to the vacant axial sites on Cu^{2+}. This much less favorable interaction of water molecules in the axial directions is due to the double occupation of the Cu^{2+} $3d_{z^2}$ orbital effectively screening the positive charge on the metal ion.

Our results corroborate a transition from more open geometries in the gas phase to more compact 3-D hydrogen-bonded structures in the aqueous phase. The five-coordinate square-pyramidal geometry is found to be the most stable structure in the solvation phase ($n \geq 8$). For clusters in which copper(II) is fully solvated in water ($n = 16, 18$), a preference for 5-fold coordinated geometry is confirmed by analyzing potential energy curves for displacement of axial water molecules to the second hydration shell. However, the differences between the energies of Cu(II)−water clusters with coordination number five and six are relatively small (∼1.4 kcal/mol) suggesting that both forms may coexist in solution. These results are consistent with the combined EXAFS and XANES studies of aqueous solutions of Cu(II) by Frank and co-workers.[20] Mixed cluster/continuum models that include at least two full solvation shells can be an important tool for determining accurate structural parameters and coordination numbers of metal ions in aqueous solutions, particularly when different experimental and theoretical techniques reach different conclusions regarding the structure of hydrated ions.[97]

The hydration free energy of Cu^{2+} calculated using the mixed cluster/continuum approach (−509.0 kcal/mol) is in excellent agreement with the experimental value (507.0 ± 4.0 kcal/mol). To obtain such accurate solvation energies, it was essential to include two full hydration shells of water molecules (to accounts for most of the charge transfer from water to Cu^{2+}).

Supporting Information Available: Cartesian coordinates and absolute energies for all $[Cu(H_2O)_n]^{2+}$ complexes optimized at the B3LYP/6-311++G(d,p) level of theory. This material is available free of charge via the Internet at http://pubs.acs.org.

References and Notes

(1) Adman, E. T. *Adv. Protein Chem.* **1991**, *42*, 145.

(2) Pufahl, R. A.; Singer, C. P.; Peariso, K. L.; Lin, S.-J.; Schmidt, P. J.; Fahrni, C. J.; Culotta, V. C.; Penner-Hahn, J. E.; O'Halloran, T. V. *Science* **1997**, *278*, 853.

(3) Culotta, V. C.; Klomp, L. W.; Strain, J.; Casareno, R. L.; Krems, B.; Giltin, J. D. *J. Biol. Chem.* **1997**, *272*, 23469.

(4) Hazes, B.; Magbus, K. A.; Bonaventura, C.; Bonaventura, J.; Dauter, Z.; Kalk, K. H.; Hol, W. G. *Protein Sci.* **1993**, *2*, 597.

(5) Solomon, E. I.; Szilagyi, R. K.; George, S. B.; Basumallick, L. *Chem. Rev.* **2004**, *104*, 419.

(6) Katz, A. K.; Shimoni-Livny, L.; Navon, O.; Bock, C. W.; Glusker, J. P. *Helv. Chim. Acta* **2003**, *86*, 1320.

(7) Halcrow, M. A. *Dalton Trans.* **2003**, 4375.

(8) Sabolovic, J.; Liedl, K. R. *Inorg. Chem.* **1999**, *38*, 2764.

(9) Sabolovic, J.; Tautermann, C. S.; Loerting, T.; Liedl, K. R. *Inorg. Chem.* **2003**, *42*, 2268.

(10) Deeth, R. J.; Hearnshaw, L. J. A. *Dalton Trans.* **2006**, 1092.

(11) Chaurin, V. C.; Constable, E. C.; Housecroft, C. E. *New J. Chem.* **2006**, *30*, 1740.

(12) Weiss, R.; Jansen, G.; Boese, R.; Epple, M. *Dalton Trans.* **2006**, 1831.

(13) Persson, I.; Persson, P.; Sandström, M.; Ullström, A.-S. *J. Chem. Soc., Dalton, Trans.* **2002**, 1256.

(14) Shapovalov, I. M.; Radchenko, I. V. *Zh. Struct. Khim.* **1971**, *12*, 769.

(15) Magini, M. *Inorg. Chem.* **1982**, *21*, 1535.

(16) Sheals, J.; Persson, P.; Hedman, B. *Inorg. Chem.* **2001**, *40*, 4302.

(17) Tran, M. L.; Gahan, L. R.; Gentle, I. R. *Phys. Chem. B* **2004**, *108*, 20130.

(18) Benfatto, M.; D'Angelo, P.; Longa, S. D.; Pavel, N. V. *Phys. Rev. B* **2002**, *65*, 174205.

(19) Chaboy, J.; Muñoz-Páez, A.; Merkling, P. J.; Marcos, E. S. *J. Chem. Phys.* **2006**, *124*, 064509.

(20) Frank, P.; Benfatto, M.; Szilagyi, R. K.; D'Angelo, P.; Longa, S. D.; Hodgson, K. O. *Inorg. Chem.* **2005**, *44*, 1922.

(21) Åkesson, R.; Pettersson, L. G. M.; Sandström, M.; Wahlgren, U. *J. Am. Chem. Soc.* **1994**, *116*, 8691.

(22) Åkesson, R.; Pettersson, L. G. M.; Sandström, M.; Wahlgren, U. *J. Am. Chem. Soc.* **1994**, *116*, 8705.

(23) Bertrán, J.; Rodrígues-Santiago, L.; Sodupe, M. *J. Phys. Chem. B* **1999**, *103*, 2310.

(24) Bèrces, A.; Nukada, T.; Margl, P.; Ziegler, T. *J. Phys. Chem. A* **1999**, *103*, 9693.

(25) Rulíšek, L.; Havlas, Z. *J. Am. Chem. Soc.* **2000**, *122*, 10428.

(26) Pushie, M. J.; Rauk, A. *J. Biol. Inorg. Chem.* **2003**, *8*, 53.

(27) Pavelka, M.; Burda, J. V. *Chem. Phys.* **2005**, *312*, 193.

(28) Tarazona-Vasquez, F.; Balbuena, P. B. *J. Phys. Chem. B* **2005**, *109*, 12480.

(29) Rickard, G. A.; Gomez-Balderas, R.; Brunelle, P.; Raffa, D. F.; Rauk, A. *J. Phys. Chem. A* **2005**, *109*, 8361.

(30) Hattori, T.; Toriashi, T.; Tsuneda, T.; Nagasaki, S.; Tanaka, S. *J. Phys. Chem. A* **2005**, *109*, 10403.

(31) Pasquarello, A.; Petri, I.; Salmon, P. S.; Parisel, O.; Car, R.; Tóth, É.; Powell, D. H.; Fisher, H. E.; Helm, L.; Merbach, A. E. *Science* **2001**, *291*, 856.

(32) Amira, S.; Spangberg, D.; Hermasson, K. *Phys. Chem. Chem. Phys.* **2005**, *7*, 2874.

(33) Blumberger, J.; Bernasconi, L.; Tavernelli, I.; Vuilleumier, R.; Sprik, M. *J. Am. Chem. Soc.* **2004**, *126*, 3928.

(34) Schwenk, C. F.; Rode, B. M. *Phys. Chem. Chem. Phys.* **2003**, *5*, 3418.

(35) Schwenk, C. F.; Rode, B. M. *ChemPhysChem.* **2003**, *4*, 931.

(36) Schwenk, C. F.; Rode, B. M. *J. Chem. Phys.* **2003**, *119*, 9523.

(37) Schwenk, C. F.; Rode, B. M. *J. Am. Chem. Soc.* **2004**, *126*, 12786.

(38) Figgis, B. N.; Hitchman, M. A. *Ligand Field Theory and Its Applications*; Wiley-VCH: New York, 2000.

(39) Cotton, F. A.; Wilkinson, G.; Murillo, C. A.; Bochman, M. *Advanced Inorganic Chemistry*, 6th ed.;Wiley-Interscience: New York, 1999.

(40) Jahn, H. A.; Teller, E. *Proc. R. Soc. London, Ser. A* **1937**, *161*, 220.

(41) Bersuker, I. B. *The Jahn-Teller Effect*; Cambridge University Press: Cambridge, 2006.

(42) Powell, D. H.; Helm, L.; Merbach, A. E. *J. Chem. Phys.* **1991**, *95*, 9258.

(43) Powell, D. H.; Furrer, P.; Pittet, P.-A.; Merbach, A. E. *J. Phys. Chem.* **1995**, *99*, 16622.

(44) Stace, A. J. *Phys. Chem. Chem. Phys.* **2001**, *3*, 1935.

(45) Walker, N. R.; Firth, S.; Stace, A. J. *J. Am. Chem. Soc.* **1997**, *119*, 10239.

(46) Walker, N. R.; Firth, S.; Stace, A. J. *Chem. Phys. Lett.* **1998**, *292*, 125.

(47) Duncombe, B. J.; Duale, K.; Buchanan-Smith, A.; Stace, A. J. *J. Phys. Chem. A* **2007**, *111*, 5158.

(48) Klamt, A.; Schüürmann, G. *J. Chem. Soc., Perkin Trans. 2* **1993**, 799.

(49) *Jaguar, version 7.0*; Schrödinger LLC: New York, 2007.

(50) Becke, A. D. *Phys. Rev. A* **1988**, *38*, 3098.

(51) Lee, C. T.; Yang, W. T.; Parr, R. G. *Phys. Rev. B* **1988**, *37*, 785.

(52) Peschke, M.; Blades, A. T.; Kebarle, P. *J. Am. Chem. Soc.* **2000**, *122*, 10440.

(53) Marino, T.; Toscano, M.; Russo, N.; Grand, A. *J. Phys. Chem. B* **2006**, *110*, 24666.

(54) Tunell, I.; Lim, C. *Inorg. Chem.* **2006**, *45*, 4811.

(55) Carl, D. R.; Moision, R. M.; Armentrout, P. B. Int. *J. Mass Spectrom.* **2007**, *265*, 308.

(56) Bertrán, J.; Rodriguez-Santiago, L.; Sodupe, M. *J. Phys. Chem. B* **1999**, *103*, 2310.

(57) Poater, J.; Solá, M.; Rimola, A.; Rodríguez-Santiago, L.; Sodupe, M. *J. Phys. Chem. A* **2004**, *108*, 6072.

(58) Georgieva, I.; Trendafilova, N.; Rodríguez-Santiago, L.; Sodupe, M. *J. Phys. Chem. A* **2005**, *109*, 5668.

(59) Rimola, A.; Rodríguez-Santiago, L.; Sodupe, M. *J. Phys. Chem. B* **2007**, *111*, 5740.

(60) Hay, P. J.; Wadt, W. R. *J. Chem. Phys.* **1985**, *82*, 299.

(61) Jaguar, version 7.0, User Manual.

(62) Kendall, R. A.; Dunning, T. H., Jr.; Harrison, R. J. *J. Chem. Phys.* **1992**, *96*, 6796.

(63) Li, J.; Fisher, C. L.; Chen, J. L.; Bashford, D.; Noodleman, L. *Inorg. Chem.* **1996**, *35*, 4694.

(64) Rotzinger, F. P. *J. Am. Chem. Soc.* **1997**, *119*, 5230.

(65) Martin, R. L.; Hay, J. P.; Pratt, L. R. *J. Phys. Chem. A* **1998**, *102*, 3565.

(66) Tawa, G. J.; Topol, I. A.; Burt, S. K.; Caldwell, R. A.; Rashin, A. A. *J. Chem. Phys.* **1998**, *109*, 4852.

(67) Mejias, J. A.; Lago, S. *J. Chem. Phys.* **2000**, *113*, 7306.

(68) Pliego, J. R., Jr.; Riveros, J. M. *J. Phys. Chem. A* **2001**, *105*, 7241.

(69) Zhan, C.-G.; Dixon, D. A. *J. Phys. Chem. A* **2001**, *105*, 11534.

(70) Zhan, C.-G.; Dixon, D. A. *J. Phys. Chem. A* **2002**, *106*, 9737.

(71) Pliego, J. R., Jr.; Riveros, J. M. *J. Phys. Chem. A* **2002**, *106*, 7434.

(72) Asthagiri, D.; Pratt, L. R.; Ashbaugh, H. S. *J. Chem. Phys.* **2003**, *119*, 2702.

(73) Uudsemaa, M.; Tamm, T. *J. Phys. Chem. A* **2003**, *107*, 9997.

(74) Uudsemaa, M.; Tamm, T. *Chem. Phys. Lett.* **2004**, *400*, 54.

(75) Zhan, C.-G.; Dixon, D. A. *J. Phys. Chem. A* **2004**, *108*, 2020.

(76) Asthagiri, D.; Pratt, L. R.; Paulaitis, M. E.; Rempe, S. B. *J. Am. Chem. Soc.* **2004**, *126*, 1285.

(77) Kelly, C. P.; Cramer, C. J.; Truhlar, D. G. *J. Chem. Theory Comput.* **2005**, *1*, 1133.

(78) Rode, B. M.; Schwenk, C. F.; Hofer, T. S.; Randolf, B. R. *Coord. Chem. Rev.* **2005**, *249*, 2993.

(79) Kelly, C. P.; Cramer, C. J.; Truhlar, D. G. *J. Phys. Chem. B* **2006**, *110*, 16066.

(80) Kelly, C. P.; Cramer, C. J.; Truhlar, D. G. *J. Phys. Chem. A* **2006**, *110*, 2493.

(81) De Abreu, H. A.; Guimaraes, L.; Duarte, H. A. *J. Phys. Chem. A* **2006**, *110*, 7713.

(82) Gutowski, K. E.; Dixon, D. A. *J. Phys. Chem. A* **2006**, *110*, 8840.

(83) Wiebke, J.; Moritz, A.; Cao, X.; Dolg, M. *Phys. Chem. Chem. Phys.* **2007**, *9*, 459.

(84) Jaque, P.; Marenich, A. V.; Cramer, C. J.; Truhlar, D. G. *J. Phys. Chem. C* **2007**, *111*, 5783.

(85) Bryantsev, V. S.; Diallo, M. S.; Goddard, W. A., III. *J. Phys. Chem. B* **2008**,*112*,9709.

(86) Ahlrichs, R.; Bär, M.; Häser, M.; Horn, H.; Kölmel, C. *Chem. Phys. Lett.* **1989**, *162*, 165.

(87) Klamt, A.; Jonas, V.; Bürger, T.; Lohrenz, C. W. *J. Phys. Chem. A* **1998**, *102*, 5074.

(88) Tannor, D. J.; Marten, B.; Murphy, R.; Friesner, R. A.; Sitkoff, D.; Nicholls, A.; Ringnalda, M.; Goddard, W. A., III; Honig, B. *J. Am. Chem. Soc.* **1994**, *116*, 11875.

(89) Bondi, A. *J. Chem. Phys.* **1964**, *64*, 441.

(90) O'Brien, J. T.; Williams, E. R. *J. Phys. Chem. A* **2008**, *112*, 5893.

(91) Su, J. T.; Xu, X.; Goddard, W. A., III. *J. Phys. Chem. A* **2004**, *108*, 10518.

(92) Glendening, E. D.; Badenhoop, J. K.; Reed, A. E.; Carpenter, J. E.; Bohmann, J. A.; Morales, C. M.; Weinhold, F. NBO; Theoretical Chemistry Institute, University of Wiscosin, Madison, WI, 2001; http://www.chem. wisc.edu/~nbo5.

(93) Reed, A. E.; Curtiss, L. A.; Weinhold, F. *Chem. Rev.* **1988**, *88*, 899.

(94) Siboulet, B.; Marsden, C. J.; Vitorge, P. *Chem. Phys.* **2006**, *326*, 289.

(95) Marcus, Y. *Ion Solvation*; Wiley: New York, 1985.

(96) Tissandier, M. D.; Cowen, K. A.; Feng, W. Y.; Gundlach, E.; Cohen, M. H.; Earhart, A. D.; Coe, J. V. *J. Phys. Chem. A* **1998**, *102*, 7787.

(97) Varma, S.; Rempe, S. B. *Biophys. Chem.* **2006**, *124*, 192.

JP804373P